Liquid crystals of polyelectrolyte networks

R. Bruinsma
Physics and Astronomy Department, University of California, Los Angeles, California 90024
(Received 23 May 2000; published 21 May 2001)

The Onsager theory of nematic liquid crystals is extended to rigid polyelectrolytes cross-linked by polyvalent ions. Recent synchrotron x-ray diffraction experiments showed that dilute, birefringent networks are formed under these conditions. The application of Onsager theory to this system leads to the prediction of the existence of a range of exotic mesophases such as the ''cubatic,'' the ''tetratic,'' and the ''trigatic.'' The exotic network phases appear on the border of regions of phase coexistence of network phase with isotropic material (at low polyvalent ion concentration) and with dense bundles (at high polyvalent ion concentration).

DOI: 10.1103/PhysRevE.63.061705 PACS number(s): 87.15.−v, 61.30.Cz, 64.70.Md

I. INTRODUCTION

Rodlike organic molecules can align spontaneously and develop nematic liquid-crystalline order. In his classical paper of 1949 [1], Onsager showed that the critical volume fraction of cylindrical rods required for the onset of nematic order in a solution of long rods is very low, and is of the order of the aspect ratio D/L of the rods (with D the rod diameter and L the rod length). Onsager theory applies only to molecules in good solvent. Early studies of the effects of reduced solvent quality on solutions of stiff synthetic polymers reported that some form of aggregation took place [2], and it was suggested that these aggregates might be dense bundles of rods [3].

The phase behavior of biopolymers has recently received considerable attention, in particular that of the long, stiff, biopolymer actin, a major ingredient of muscles and of the cytoskeleton of cells [4]. As a function of rod concentration, solutions of stabilized actin filaments exhibit an isotropic-to-nematic transition [5]. The onset concentration of about 2 mg/ml (for long molecules) agrees well with Onsager theory provided one uses for L the persistence length [6] (of order 10 μm for actin). When so-called ''linker proteins'' are added to actin solutions, dense bundles can be observed (known as ''stress fibers'') as well as gel-like networks [7]. As a function of linker concentration, actin solutions show a sol-gel transition [8] where the viscosity diverges. At higher linker concentrations, microphase separation takes place, characterized by strong light scattering and eventually bundles appear. A schematic phase diagram is shown in Fig. 1. The elastic properties of linked actin networks have been examined extensively [9], although the theoretical interpretation remains somewhat controversial [10]. Both the actin bundles and the actin networks are encountered in the cytoplasm of cells and the fact that the elastic properties of actin networks can be significantly modified by modest changes in linker concentration may play an important role in cell motility [11].

Charged biopolymers, like actin or DNA, also can be linked together by *polyvalent ions*. Because polyvalent ions are easier to describe than linker proteins, they form a suitable model system to study the physics of linking biopolymers. Bundling is observed [12] when millimolar concentrations of polyvalent ions are added to biopolymer solutions. Numerical simulations of charged rods in the presence of polyvalent ions report that the polyvalent ions generate short-range attractive forces [13], which presumably are responsible for the bundle formation. Numerical simulations of bundle formation [14] obtain modest bundle diameters (10–50 rods) probably due to kinetic effects [15].

The present paper was motivated by a recent low-angle synchrotron x-ray study [16] that was performed on actin solutions in the presence of low concentrations of Ca^{2+} and Sr^{2+}. A gel-like network phase was observed at low ion concentrations. For example, for 10 μm actin rods in the presence of Ca^{2+} ions, a network phase appeared around 10 mM which extended over a range of 5 mM, while dense bundles came in at about 25 mM. The surprising result was that this network phase was *birefringent* with an unusual structure factor $S(q_z,q_\perp)$. Perpendicular to the optical axis, $S(q_z=0,q_\perp)$ exhibited a sequence of well-defined peaks. From the peak position of the first maximum $q_\perp^*$, the mean spacing ξ between the rods could be deduced to be of order 200 Å. This length is large compared to the actin diameter, so the network must be dilute. The presence of higher-order harmonics indicated that there was a considerable amount of local positional order in the direction transverse to the optical axis. The most logical assumption would be that the structure factor is that of a polymer nematic [17]. However, along the optical axis, $S(q_z,q_\perp=0)$ exhibited a maximum q_z^* with a magnitude about half of that of $q_\perp^*$. This is puzzling since

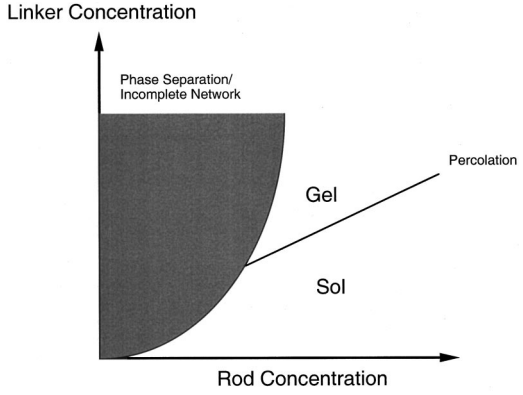

FIG. 1. Schematic phase diagram of the sol-gel transition of a mixture of rods and strong linkers.

for polymer nematics, the function $S(q_z, q_\perp = 0)$ should (for small q_z) be *zero* for fundamental reasons [17]. It follows that the birefringent network phase of actin cannot be a polymer nematic. Since actin is a chiral biopolymer, one explanation might be that the q_z^* peak is associated with the pitch of a *chiral* polymer liquid crystal [18]. However, in a number of cases the longitudinal peak position was found to be definitely off the optical axis. This is fundamentally inconsistent with any form of chiral order. The interpretation of the longitudinal peak offered by the experimentalists was that *a certain fraction of the rods are oriented perpendicular to the optical axis* (for the case of the off-axis peaks, the angle would be somewhat less than 90°). The peak at q_z^* would be due to (short-range) positional order among the transverse rods.

It is important to pay close attention to the electrostatics of the system. It was proposed many years ago [19] that the phase diagram of polyelectrolyte solutions with no cross linkers might contain a curious, positionally ordered, phase with *cubic symmetry* at very low polymer concentrations (and no added salt) because electrostatic repulsion between rods should favor $\pi/2$ crossing angles. The cubic phase, which has long-range positional order, was never observed. The electrostatic torque between adjacent rods would be greatly enhanced by linkers since the linkers force the rods to be in close proximity. A pair of charged rods connected by a mobile, flexible link (such as a polyvalent ion) would tend to form a crosslike structure. Monte Carlo simulations [20] of collections of cross-shaped molecules report formation of the *cubatic* liquid-crystal phase. This phase, which had been proposed by Nelson and Toner on theoretical grounds [21], resembles the cubic structure but, although it has cubic orientational order, it lacks positional order. The cubatic has been encountered only in numerical simulations so far. It would appear suggestive that the unusual birefringent actin networks may be related to the cubic or the cubatic phase but neither of these two phases is birefringent.

The first aim of the present study is to use Onsager theory to reexamine the nature of the liquid-crystal phases of charged rods in the presence of linkers. Since Onsager theory is able to account for the formation of nematic order in actin in the absence of linkers, it is the natural starting point for an analysis of the birefringent properties of linked actin networks. Depending on the optimal crossing angle between rods, we indeed find a whole variety of exotic liquid crystals. The symmetry groups of these phases are related to certain of the point-group symmetries of the Bravais lattice, even though they lack positional order. For the specific case of 90° crossing angles, Onsager theory predicts that, apart from the conventional nematic, we should encounter two other mesophases: the cubatic phase as well as a ''tetratic'' phase [22], a cubatic with a tetragonal distortion along one of the cubic axes with the point-group symmetry of a tetragonal crystal. The appearance of the tetratic is due to competition between excluded volume effects and electrostatic torque. For crossing angles different from 90°, a variety of complex phases with different point-group symmetries may be realized.

When the ion concentration was increased in the experiments of Ref. [16], the scattering intensity decreased and $S(q_z = 0, q_\perp)$ exhibited additional peaks at larger wave vectors that could be indexed by the structure factor of a densely packed hexagonal bundle. The bundle phase and the network phase coexisted over a large range of concentrations. This offers a second puzzle: once a sufficient amount of polyvalent ions is available to start forming dense, charge-neutral bundles, why would the dilute network phase persist to higher ion concentrations? The second aim of the paper is to use a generalization of Onsager theory to understand why dense-dilute phase-coexistence phenomena appear to accompany the exotic phases and to determine what sets the characteristic length scale of the networks. Onsager theory indeed predicts that the novel phases should appear right on the border of phase-decomposition areas in the phase diagram. We find two different forms of dense-dilute phase coexistence: (i) between a linker-rich network phase and a linker-poor isotropic solution and (ii) between a linker-poor network phase and a linker-rich dense bundle phase. *Entropy* plays a central role in both cases. In the first case, entropic effects make the network compact and force the characteristic mesh size ξ of the network to be of the order of the Debye screening length. In the second case, entropy gain by the counter-ion release mechanism stabilizes the network phase and allows for an extensive region of dense bundle–dilute network phase coexistence.

II. MODEL

A. General

Assume a nonbirefringent, aqueous, semidilute solution of very long cylindrical rods of length L, diameter D (with $L \gg D$), and concentration ϕ. The cylinders are assumed to carry a negative line charge per unit length λ along their central axis exceeding the Manning threshold $\lambda = -e/l_B$, (l_B is the Bjerrum length). Under these conditions, a cloud of ''condensed'' counterions envelops the rods [23], reducing the effective charge per unit length from λ down to $-e/l_B$. The solution also contains a low concentration of monovalent ions characterized by a Debye parameter κ and a very low concentration ψ of small, positive polyvalent ions of valence Z. The Manning cloud of ions surrounding the rod is enriched in polyvalent ions since every polyvalent ion that enters the cloud allows the release of Z monovalent ions into bulk, with a corresponding lowering of the entropic free energy by, roughly, $(Z-1)k_BT$. As a result, nearly all of the polyvalent ions will be condensed on the rods under standard conditions. This means that for a homogeneous solution of ions and rods, the mean number of polyvalent ions per rod would be ψ/ϕ. We will assume homogeneity for now and postpone a discussion of decomposition phenomena to the last section. We also will assume the following.

(i) The size of the polyvalent ions is sufficiently small enough so they can be ''shared'' only between two rods at a time.

(ii) The ion-to-rod concentration ratio is considerably below the isoelectric point (the point where the charge of the polyvalent ions compensates the charge of the rods).

(iii) The Debye screening length is large compared with the rod diameter D but small compared with the rod length L (so $\kappa D \ll 1$ but $\kappa L \gg 1$).

(iv) The rod length is less than the persistence length so the polymers can be treated as rigid rods.

B. Electrostatic torque

The electrostatic potential energy per unit length $U(\gamma,R)$ of two cylindrical, charged rods passing each other with an (acute) angle γ at a minimum separation of R was computed within Debye-Hückel (DH) theory [24] by Brenner and Parsegian (BP),

$$U(\gamma,R)/k_BT = \Gamma \frac{e^{-\kappa R}}{|\sin(\gamma)|}. \tag{2.1}$$

Here Γ is a dimensionless parameter that characterizes the strength of the electrostatic repulsion as compared to k_BT. It follows from Eq. (2.1) that the electrostatic repulsion between two nearby rods produces a nonzero mutual torque $\partial U(\gamma,R)/\partial\gamma$ if the angle γ is not equal to 90°.

Equation (2.1) holds only in the absence of Manning condensation because re-arrangement of condensed counterions near a crossing site is likely to produce angle-dependent corrections to Eq. (2.1). In the presence of counter-ion condensation, the function $U(\gamma,R)$ should be qualitatively similar to Eq. (2.1), and in particular it should have a minimum at $\gamma=\pi/2$. Whenever an explicit form for $U(\gamma,R)$ is required, we will include the effects of the counterions in the usual way by replacing in the DH formula the bare charge per unit length with the Manning-renormalized charge per unit length e/l_B. This gives a value for Γ of the order of $1/\kappa l_B$ so Γ increases with decreasing salt concentration.

C. Salt bridges

A crossing site between two rods with a minimum spacing R of order D is an *electrostatic trap* for condensed polyvalent ions (see Fig. 2). The entropic free-energy cost of localizing one polyvalent ion at a crossing site salt is Z times smaller than the entropic free-energy cost of localizing an equivalent number of monovalent salt ions, so we will ignore accumulation of monovalent ions at crossing sites.

1. Single-ion salt bridge

For a crossing site with just a single localized polyvalent ion, the electrostatic energy is minimized when the polyvalent (point) ion is localized right at the geometrical center of the crossing point [see Fig. 2(a)]. Denote the two rods by 1 and 2. The electrostatic free energy gain of placing a polyvalent ion at a crossing site (that initially carried no polyvalent ion) will be denoted by $\Delta H_{\rm el}(\gamma)$, with γ the crossing angle. $\Delta H_{\rm el}(\gamma)$ is of order Zk_BT, keeping in mind that the effective charge per unit length of the rods equals e/l_B. For explicit calculations, we will assume that $\Delta H_{\rm el}$ is a constant. The entropic free energy of localizing a polyvalent ion (confined to a rod) to one particular site is of the order to $k_BT\ln(\psi l_0/\phi L)$ since $\psi/\phi L$ is the number of polyvalent ions

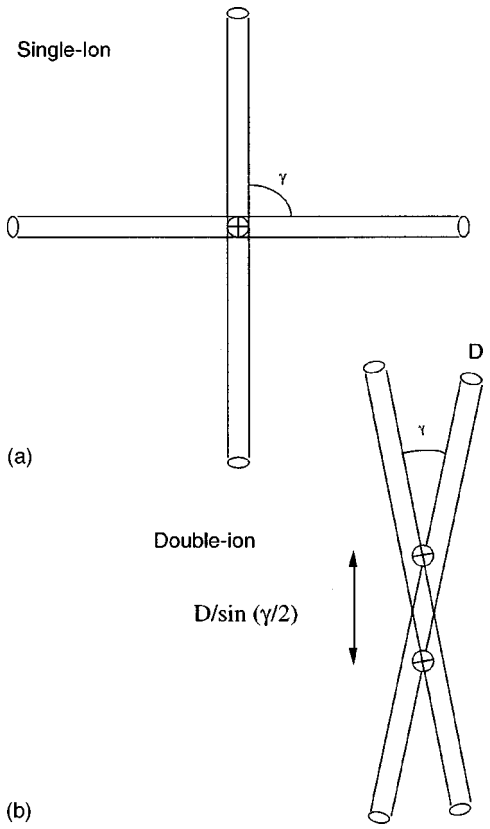

FIG. 2. Ion links between two charged rods. (a) Single-ion salt bridge. The optimal angle is 90°. (b) Two-ion salt bridge. The optimal angle is less than 90°.

per unit length (l_0 is a molecular length). The formation free energy $\Delta F_1(\gamma)$ of a single-ion bridge is the sum of these two terms minus the energy cost of bringing the two rods together, as given by Eq. (2.1),

$$\Delta F_1(\gamma) = \Delta H_{\rm el} + k_BT\ln\left(\frac{\psi l_0}{\phi L}\right) - k_BT\frac{\Gamma}{|\sin\gamma|}. \tag{2.2a}$$

2. Double-ion salt bridge

The electrostatic energy of a two-ion bridge is minimized when the two ions are arranged symmetrically on opposite sides of the crossing point along the direction of the two acute angles of the cross [see Fig. 2(b)]. The formation free energy is, approximately, twice $\Delta H_{\rm el}+k_BT\ln(\psi l_0/\phi L)$ minus the sum of the energy cost of bringing the two rods together and of bringing the two ions together. This latter term is angle-dependent and proportional to $\sin(\gamma/2)$ as follows from Fig. 2b. For explicit calculations, the formation free energy $\Delta F_2(\gamma)$ of a two-ion salt bridge with γ acute will be taken to be

$$\Delta F_2(\gamma) = 2\Delta H_{\rm el} + 2k_BT\ln\left(\frac{\psi l_0}{\phi L}\right) - \Delta\sin\left(\frac{\gamma}{2}\right) - k_BT\frac{1}{|\sin\gamma|} \tag{2.2b}$$

with Δ a dimensionless parameter of order one. The formation free energy for obtuse γ is found from the condition

$\Delta F_2(\pi-\gamma)=\Delta F_2(\gamma)$. The one important feature of Eq. (2.2b) is that, unlike $\Delta F_1(\gamma)$, the minimum of $\Delta F_2(\gamma)$ is no longer at 90° because of the Δ sin $(\gamma/2)$ term.

III. GENERALIZED ONSAGER THEORY

A. Variational free energy

Let $f_\psi(\Omega)$ be the normalized orientational distribution function, with $f_\psi(\Omega)=f_\psi(-\Omega)$. Onsager's free energy functional for $f_\psi(\Omega)$ has the following general form:

$$\beta F[f_\psi(\Omega)]/\phi \cong \ln \phi \nu_T + \int d\Omega\, f_\psi(\Omega)\ln[4\pi f_\psi(\Omega)] + \int\int d\Omega_1 d\Omega_2 f_\psi(\Omega_1) f_\psi(\Omega_2) V(\gamma_{12}). \tag{3.1}$$

The first term is the translational entropic free energy where v_T is the thermal volume and ϕ is the rod concentration. The second term is the orientational entropic free energy and the third term is the correlation energy computed within second-order virial theory. The kernel $V(\gamma)$ in Eq. (3.1) takes the form

$$V(\gamma)=\phi L^2|\sin\gamma|\left\{D-de^{\beta\Delta F(\gamma)}+\kappa^{-1}\times\left[\ln\left(\frac{\Gamma}{|\sin\gamma|}\right)+C+E_1\left(\frac{\Gamma}{|\sin\gamma|}\right)\right]\right\}. \tag{3.2}$$

The first two terms in Eq. (3.2) are, respectively, the standard Onsager excluded volume term, and the short-range interaction due to sliding linker molecules. The length scale d $(\ll D)$ is the effective range of the salt-bridge interaction. The formation free energy $\Delta F(\gamma)$ of the ion link should be equated to either $\Delta F_1(\gamma)$ or $\Delta F_2(\gamma)$, depending on whether one or two ions is involved. It is assumed that the salt-bridge can freely slide over the rods. The last term, derived by Stroobants *et al.* [6], is the contribution from the BP long-range electrostatic repulsion [see Eq. (2.1)], C is the Euler constant and $E_1(x)$ is the exponential integral. We will define the control parameter $e^{\beta\Delta F_0}$ to be the angle-independent part of the Boltzmann factor of the (single-ion) salt-bridge energy,

$$e^{\beta\Delta F_0}\equiv\frac{\psi l_0}{\phi L}e^{\beta\Delta H_{\rm el}}. \tag{3.3}$$

Since $e^{\beta\Delta F_0}$ is proportional to the ion-to-rod concentration ratio (ψ/ϕ), we will consider $e^{\beta\Delta F_0}$ as an experimentally accessible control parameter.

The structure of the function $V(\gamma)$ as a function of $e^{\beta\Delta F_0}$ will play an important role in the following. Figure 3 shows the typical form of $V(\gamma)$ for a single-ion salt bridge [using Eq. (2.2a) for $\Delta F(\gamma)$]. For low values of $e^{\beta\Delta F_0}$, $V(\gamma)$ has a primary minimum at $\gamma=0$. For κD small and Γ of order one, a secondary minimum appears at $\gamma=\pi/2$. The secondary minimum is more pronounced for larger Γ but it never be-

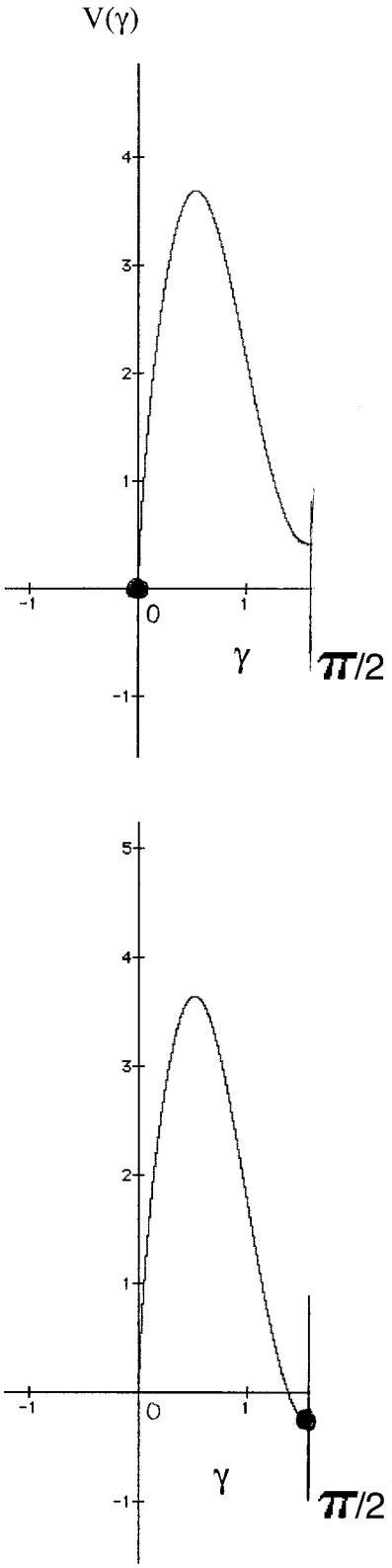

FIG. 3. Typical form of the function $V(\gamma)$ given by Eq. (3.2) for the case of a single-ion salt bridge. The function is shown for two values of $e^{\beta\Delta F_0}$ near the point where the minimum shifts from $\gamma=0$ to $\gamma=\pi/2$.

comes the primary minimum if $e^{\beta\Delta F_0}=0$ (i.e., if there are no salt bridges). For nonzero $e^{\beta\Delta F_0}$, the secondary minimum deepens, and turns into the primary minimum of $V(\gamma)$ at a critical value of $e^{\beta\Delta F_0}$ of order D/d.

To obtain a better insight into the implications of this shift in the position of the absolute minimum of $V(\gamma)$, assume that the correlation energy is the dominant term of Eq. (3.1). The problem is then to determine what orientational distribution minimizes the correlation energy under the condition that $f_\psi(\Omega)$ is normalized over the unit sphere. If the absolute minimum of $V(\gamma)$ is at $\gamma=0$, then the correlation energy is minimized by a function $f_\psi(\Omega)$ that is highly peaked along a particular direction. This corresponds to the nematic phase. The alignment is due to the excluded volume effect. Next, suppose that $V(\gamma)$ is of the form shown in Fig. 3 with the absolute minimum at $\gamma=\pi/2$. The correlation energy then is minimized by a function $f_\psi(\Omega)$ that has equal-sized peaks along three orthogonal directions, i.e., by a function $f_\psi(\Omega)$ with cubic symmetry, which corresponds to the Nelson-Toner cubatic phase. This argument would lead us to expect a first-order phase transition from a nematic phase to a cubatic phase as a function of the control parameter $e^{\beta\Delta F_0}$. The scenario is not very sensitive to the detailed shape of $V(\gamma)$: it only requires that a second minimum in $V(\gamma)$ develops at $\gamma=\pi/2$ as a function of the control parameter $e^{\beta\Delta F_0}$.

For the case of a *two-ion* salt bridge, the second minimum of $V(\gamma)$ appears at some angle γ^* less than $\pi/2$ [see Eq. (2.2b)]. Obtaining the orientational distribution $f_\psi(\Omega)$ minimizing the correlation free energy is a less trivial mathematical problem in this case. If the second minimum of $V(\gamma)$ at γ^* has just turned into the absolute minimum of $V(\gamma)$, then minimizing the correlation energy leads to a $f_\psi(\Omega)$ that consists of a number of preferred directions on the unit sphere such that the angle subtended between pairs of directions is equal to γ^* or to $\pi-\gamma^*$. There are a number of different ways how this can be arranged.

1. Planar structures

The simplest case is when the rod orientations are restricted to a *plane* [see Fig. 4(a)]. For arbitrary γ^*, an obvious choice for $f_\psi(\Omega)$ would consist of two preferred directions that make a mutual angle γ^*. This corresponds to a two-dimensional nematic liquid crystal. The optical axis is the bisector of the two peak directions. If planar structures also would be favorable in three dimensions, then formation of a *smectic-C* phase may be possible. A special case is obtained when γ^* is equal to 60° since then there are not two but *three* planar directions with all subtended angles equal to 60° (along the edges of an equilateral triangle). This corresponds to a (non-birefringent) hexatic liquid crystal [see Fig. 4(b)].

2. Three-dimensional structures

The simplest distribution that obeys the required condition in three dimensions is an $f_\psi(\Omega)$ that consists of three peaks along three directions Ω_i on the unit sphere making mutual angles equal γ^*. This phase is in general birefringent with the optical axis along the vector sum of the three directions. It is, however, not a nematic liquid crystal since the phase lacks uniaxial rotational invariance around the optical axis. In the most general case, the point-group symmetry of this phase is that of the Bravais lattice of the trigonal crystal so we might call it a ''trigatic'' phase. The trigatic phase can be shown to have a lower correlation free energy than the planar nematic phase. Adding peaks (e.g., by forming a triangular lattice of peaks on the unit sphere) increases the correlation free energy and is in general not favorable. However, as for the two-dimensional case, for certain special values of γ^*, the correlation energy can be further reduced by adding more peaks. For instance, for $\cos\gamma^*=\frac{1}{2}$ the optimal distribution has six peaks directed along the edges of a tetrahedron while for $\cos\gamma^*=\frac{1}{3}$, the orientational distribution has four peaks directed along the four-body diagonals of the cube. Neither of these two interesting phases are, however, birefringent.

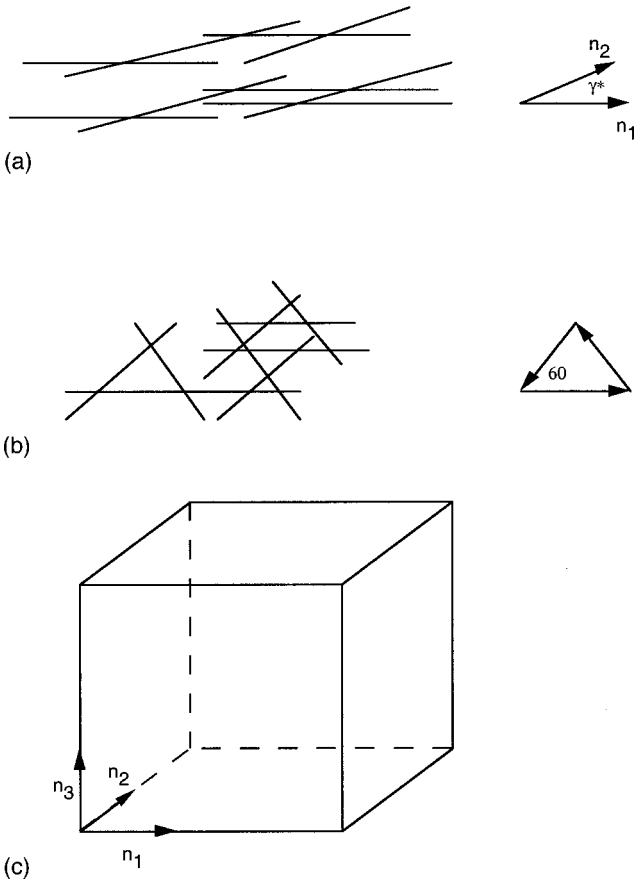

FIG. 4. Mesophases are formed by aligning rods along preferred directions that make a relative angle equal to the optimal angle γ^*. In two dimensions, there are in general two preferred directions and in three dimensions there are in general three preferred directions [(a) and (c)]. For certain special angles, there can be more preferred directions such as $\gamma^*=60°$ in two dimensions (b).

The preceding discussion applies only if the minimum at γ^* has just turned negative. If the minimum deepens then a variety of other complex structures may become possible, for instance those associated with the directions along the edges of a regular polyhedral network covering a sphere (i.e., the platonic solids) or triangular lattices on the unit sphere. For

simplicity, we will consider below only the case that the second minimum of $V(\gamma)$ is at $\gamma^* = \pi/2$, i.e., the cubatic case shown in Fig. 4(c).

B. Phase diagram

To construct the full phase diagram, we must minimize the complete free-energy equation (3.1) keeping account not only of the correlation free energy but also of the entropic term.

1. Isotropic phase

The isotropic distribution function is $f_\psi(\Omega) = 1/4\pi$. The associated variational free energy is

$$\beta F_{\rm iso}(\phi) = \phi \ln \phi \nu_T + \tfrac{1}{2}\, \phi^2 L^2 D_0 g_0 , \tag{3.4}$$

with

$$g_0 = \frac{\pi}{2} - (d/D_0) e^{\beta \Delta F_0} \int_0^\pi d\gamma \sin^2 \gamma e^{-\Gamma/|\sin(\gamma)|}, \tag{3.5a}$$

$$D_0 = D + \kappa^{-1}\left(\frac{2}{\pi}\right) \int_0^\pi d\gamma \sin^2 \gamma \times \left[\ln\left(\frac{\Gamma}{|\sin\gamma|}\right) + C + E_1\left(\frac{\Gamma}{|\sin\gamma|}\right)\right]. \tag{3.5b}$$

This quantity g_0 is a dimensionless parameter that does not depend on the rod concentration or on the rod length L and that can be considered as a second-order virial coefficient while D_0 is a renormalized rod diameter.

For increasing values of $e^{\beta \Delta F_0}$, g_0 turns negative at some critical value. The required linker concentration in order for g_0 to be zero is proportional to ϕ and independent of L. Negative values of g_0 in Eq. (3.4) are associated with negative second-order virial coefficients and hence with *phase separation.* A necessary, although not sufficient, condition of phase stability of an isotropic solution is that the second derivative of the free energy with respect to the concentration ϕ is positive. If that condition is violated, spontaneous phase separation is expected to take place. It follows from Eq. (3.4) that spontaneous phase separation happens for rod concentrations ϕ in excess of

$$\phi_I \cong \frac{1}{L^2 D_0 (-g_0)}. \tag{3.6}$$

2. Nematic phase

The Onsager trial distribution function for a nematic is of the form

$$f_O(\theta, \alpha) = \text{const} \times \cosh(\alpha \cos\theta). \tag{3.7}$$

The parameter $1/\alpha$ is proportional to the second moment $\langle \theta^2 \rangle$ of the angular distribution, and acts as a variational parameter. For conventional Onsager theory, this trial function leads to an isotropic-to-nematic transition for $\phi L^2 D$ of order 4.0. At the critical point, α is large compared to one.

Inserting Eq. (3.7) into Eq. (3.1), and minimizing the free energy with respect to α, we find that the variational free energy of the nematic is in fact not significantly affected by the presence of linkers. For $\phi L^2 D$ large compared to one, it is

$$\beta F_O(\phi) = \phi \ln(\phi \nu_T) + d_1 \phi \ln(d_2 \phi L^2 D_2) \tag{3.8}$$

with d_{1-2} positive and dimensionless and with D_2 a renormalized rod diameter D [defined similar to Eq. (3.5b)]. The contribution coming from the linkers is largely suppressed by the factor $e^{-\Gamma/\sin(\gamma)}$ since γ is small for large α. Because the second-virial term of the free energy of the *isotropic* phase is lowered by the introduction of the links—by an amount proportional to the control parameter $e^{\beta \Delta F_0}$—it follows that the isotropic-to-nematic transition point is shifted to higher values of $\phi L^2 D$ when $e^{\beta \Delta F_0}$ increases. If we increase $e^{\beta \Delta F_0}$ to the point where $g_0 = 0$, then, for large $\phi L^2 D$, the nematic phase has a higher free energy than the isotropic phase, as can be seen by comparing Eqs. (3.4) and (3.8). The critical value of $\phi L^2 D$ for the isotropic/nematic transition point in fact diverges at $g_0 = 0$,

$$(\phi L^2 D)_{IN} \propto \left(\frac{-2 \ln g_0}{g_0}\right). \tag{3.9}$$

3. Cubatic phase

For the cubatic phase we will use as our trial distribution function not one but three normalized ''Onsager-type'' angular distributions along the three preferred orthogonal directions $\hat{n}_i$ (the x, y, and z directions of a Cartesian coordinate system),

$$f = \frac{1}{3}\left\{ \sum_{i=1}^{3} f_O(\theta_i, \alpha) \right\}. \tag{3.10}$$

The $\frac{1}{3}$ prefactor is required to maintain normalization. The angle θ_i is measured from the unit vector $\hat{n}_i$, while α is to be treated again as a variational parameter. Inserting Eq. (3.10) into Eq. (3.1) and minimizing the free energy with respect to α gives the following result:

$$\beta F_C(\phi) \cong 3 \beta F_O(\phi/3) + \phi^2 L^2 D g_0^* , \tag{3.11}$$

where

$$g_0^* = \tfrac{1}{3}\{1 + [1/(D\kappa)][\ln\Gamma + C + E_1(\Gamma)] - (d/D) e^{\beta \Delta F_0 - \Gamma}\}. \tag{3.12}$$

The first term on the right-hand side of Eq. (3.11) is the Onsager free energy of a collection of three nematic phases, each having a concentration $\phi/3$, along the three preferred directions. The second term is the interaction energy between rods having different preferred directions. This second term is of the form of a second-virial term, as in Eq. (3.4) so we can identify the line $g_0^* = 0$ as a line in the phase-diagram bordering where the phase-decomposition of the cubatic

phase. Comparing Eqs. (3.5) and (3.12) we find that, as a function of increasing $e^{\beta\Delta F_0}$, the line $g_0^*=0$ is encountered before we reach $g_0=0$.

For $e^{\beta\Delta F_0}=0$, the variational free energy of the nematic phase is lower than that of the cubatic phase. For increasing $e^{\beta\Delta F_0}$, the cubatic free energy drops with respect to the nematic free energy because g_0^* decreases with $e^{\beta\Delta F_0}$ [see Eq. (3.12)] while the nematic energy is not affected by $e^{\beta\Delta F_0}$ (to lowest order). As long as g_0^* remains positive, the cubatic free energy exceeds the nematic free energy in the limit of large values of $\phi L^2 D$ [see Eqs. (3.8) and (3.11)]. At the point $g_0^*=0$, the variational free energy of the cubatic $F_C(\phi)$ equals $3F_O(\phi/3)$, according to Eq. (3.11). Because the Onsager variational free energy is a *convex* function of the concentration ϕ for larger values of $\phi L^2 D$ [see Eq. (3.8)] it follows that $3F_O(\phi/3)$ is less than $F_O(\phi)$. This means that along the line $g_0^*=0$, the cubatic must have a lower free energy than the nematic for large values of $\phi L^2 D$. The critical value of $\phi L^2 D$ for the cubatic-to-nematic transition diverges when we approach the $g_0^*=0$ line (as $1/g_0^*$). For negative values of g_0^*, we encounter a spinodal line for spontaneous phase separation of the same form as Eq. (3.6). A schematic phase diagram is shown in Fig. 5.

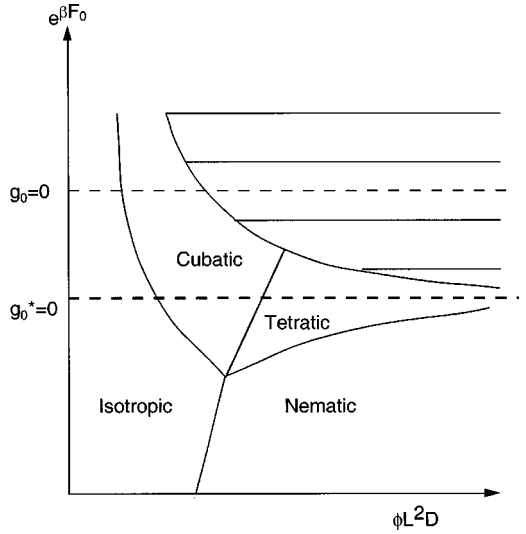

FIG. 5. Mean-field phase diagram (schematic). The vertical axis is the control parameter $e^{\beta\Delta F_0}$. The horizontal axis is the dimensionless rod concentration. The dashed lines indicate where the second-virial coefficients of the isotropic phase, respectively, the cubatic phase changes sign ($g_0=0$, respectively, $g_0^*=0$). The hatched region is the boundary for phase separation.

C. Order-parameter theory

To obtain a better insight into the competition between nematic and cubatic order near this multicritical point, we will expand $f_\psi(\Omega)$ in a series of spherical harmonic [25] and treat the expansion coefficients as order parameters for the various transitions. We thus start with

$$f_\psi(\Omega)=\frac{1}{4\pi}+\sum_{l=1}^{\infty}\sum_{m=-l}^{l}A_{l,m}Y_l^m(\theta,\varphi). \tag{3.13}$$

Since the angular distribution function must be real, we demand that $A_{l,m}=(A_{l,-m})^*$ while for achiral rods with cylindrical symmetry we may restrict l and m to even values [26]. Expanding the free energy in terms of the $A_{l,m}$ coefficients, using the completeness property of Legendre polynomials and the addition theorem for spherical harmonics, gives to second order in the $A_{l,m}$ coefficients,

$$\beta F\cong\beta F_O(\phi)+2\pi\phi\left\{\sum_{l,m}(1+\phi L^2 D_l g_l)|A_{l,m}|^2+O(A^3)\right\}. \tag{3.14}$$

In Eq. (3.14), the g_l are dimensionless parameters similar to the second-virial parameters encountered in Sec. III B, while the D_1 parameters are renormalized rod radii. More precisely,

$$g_l=\int_0^\pi d\theta\,P_l(\cos\theta)\sin^2\theta(1-(d/D_1)e^{\beta\Delta F(\theta)}), \tag{3.15a}$$

$$D_l=D+\kappa^{-1}\left\{\frac{\int_0^\pi d\theta\,P_l(\cos\theta)\sin^2\theta\left[\ln\left(\frac{\Gamma}{\sin\theta}\right)+C+E_1\left(\frac{\Gamma}{\sin\theta}\right)\right]}{\int_0^\pi d\theta\,P_l(\cos\theta)\sin^2\theta}\right\}. \tag{3.15b}$$

The higher-order terms in Eq. (3.14) all are due to the nonlinear dependence of the first (entropic) term of Eq. (3.1) on $f_\psi(\Omega)$. It follows that the coefficients of the higher-order terms in Eq. (3.14) are numerical factors that do not depend on physical quantities. The dependence of the free energy on the material parameters L, D, and ϕ thus proceeds entirely through the g_l parameters. The isotropic phase is unstable if $1+\phi L^2 D_l g_l$ is negative for any l because in that case we can reduce the free energy below that of the isotropic phase by allowing spontaneous development of a mode of the distribution function with the symmetry of a spherical harmonic with indices (l, m). The lines in the phase diagram defined by

$$\phi_l=\frac{1}{L^2 D_l(-g_l)} \tag{3.16}$$

thus determine a set of spinodal lines. For instance, Eq. (3.6) is a special case of Eq. (3.16) for $l=0$ (spontaneous growth of concentration fluctuations). Similarly, the $l=2$ case is the

instability line for spontaneous development of nematic order with $A_{20} \propto \int d\Omega\, f_\phi(\Omega) Y_2^0(\Omega)$, the usual nematic order parameter. The $l=4$ case will be seen to correspond to the development of cubatic order. To obtain the actual phase diagram near the multicritical point, we must include the nonlinear terms of Eq. (3.14). We will do this in a number of steps.

1. Nematic order

If we only allow terms of $l=2$ symmetry, then the free energy assumes the following form:

$$\frac{\beta F_2}{2\pi\phi} \cong \Big(r_2[|A_{2,0}|^2 + 2|A_{2,2}|^2] - \frac{4}{21}(\sqrt{5\pi}) \times [(A_{2,0})^3 - 6A_{2,0}|A_{2,2}|]^2 + \frac{30\pi}{21} \times \{(A_{2,0})^4 + 4|A_{2,2}|^4 + 4|A_{2,2}|^2 (A_{2,0})^2\} \Big), \tag{3.17}$$

where we included terms up to fourth order in the expansion coefficients. The parameter $r_2 = 1 + \phi L^2 D_2 g_2$ measures the distance from the $l=2$ spontaneous instability line as given by Eq. (3.16). When we decrease r_2, two nontrivival degenerate minima appear. At a first-order nematic-to-isotropic phase transition point (near $r_2 = 0.031$), these two nontrivial minima turn into the absolute minima. The first minimum has a nonzero value of $A_{2,0}$ (about 0.086 at the transition point) while $A_{2,2}=0$. We may make the standard identification of $A_{2,0}$ as the nematic order parameter. For the second minimum, both $A_{2,0}$ and $A_{2,2}$ are nonzero but this is actually not a separate case since the two orientational distributions turn out to be related by a 90° rotation.

2. Cubatic order

If we only allow terms of $l=4$ symmetry, then the free energy assumes a more complex form,

$$\begin{aligned} \frac{\beta F_4}{2\pi\phi} = {} & r_4\{(A_{4,0})^2 + 2|A_{4,2}|^2 + 2|A_{4,4}|^2\} - 9\sqrt{\pi} \\ & \times \Big\{ \frac{36}{1001}(A_{4,0})^3 - \frac{12}{191} A_{4,0}|A_{4,2}|^2 + \frac{24}{143} A_{4,0}|A_{4,4}|^2 \\ & + \frac{12}{143}\sqrt{\frac{45}{14}}[A_{4,4}(A_{4,2})^* + \text{c.c.}] \Big\} + 27\pi \\ & \times \Big\{ \frac{1058}{17\,017} A_{4,0}^4 + 12\frac{362}{21\,879} A_{4,0}^2 |A_{4,4}|^2 \\ & + 6\frac{3734}{153\,153} A_{4,0}^2 |A_{4,2}|^2 + 6\frac{5900}{153\,153}|A_{4,2}|^4 \\ & + 6\frac{980}{21\,879}|A_{4,4}|^4 + 12\frac{410}{21\,879}|A_{4,4}|^2|A_{4,2}|^2 \\ & + 12\frac{80}{17\,017}\sqrt{\frac{14}{45}}[A_{4,0}A_{4,-4}(A_{4,2}^*)^2 + \text{c.c.}] \Big\}. \end{aligned} \tag{3.18}$$

Here, $r_4 = 1 + \phi L^2 D_4 g_4$ measures the distance from the $l=4$ instability line given by Eq. (3.16). Numerical minimization with respect to the expansion parameters shows that the $A_{4,2}$ coefficients are zero within the numerical precision of the minimization.

A ''polar coordinate'' representation simplifies this free energy considerably. We define

$$\begin{aligned} A\cos\varphi &= A_{4,0}, \\ A\sin\varphi &= \sqrt{2}A_{4,4}. \end{aligned} \tag{3.19}$$

In terms of the polar A-φ variables, we can write the free energy as

$$\frac{\beta F_4(A,\varphi)}{2\pi\phi} = r_4 A^2 + F(\varphi)A_3 + G(\varphi)A^4. \tag{3.20}$$

In Eq. (3.20)

$$F(\varphi) = -9\sqrt{\pi}\left\{ \frac{36}{1001}(\cos\varphi)^3 + \frac{12}{143}\cos\varphi(\sin\varphi)^2 \right\} \tag{3.21}$$

and

$$G(\varphi) = 27\pi\left\{ \frac{1058}{17\,017}(\cos\varphi)^4 + 6\frac{362}{21\,879}(\cos\varphi)^2(\cos\varphi)^2 + \left(\frac{3}{2}\right)\frac{980}{21\,879}(\sin\varphi)^4 \right\} \tag{3.22}$$

are two dimensionless functions of the polar angle φ. $F(\varphi)$ and $G(\varphi)$ both have a single minimum at the ''magical'' angle $\varphi^* = \arctan\sqrt{\frac{5}{7}}$. The physical meaning of this angle is obtained by plotting the corresponding angular distribution function,

$$f_\psi(\Omega) = \frac{1}{4\pi} + A\{(\cos\varphi)Y_4^0(\theta,\varphi) + (\sin\varphi) \times [Y_4^4(\theta,\varphi-\varphi_0) + Y_4^{-4}(\theta,\varphi-\varphi_0)/\sqrt{2}]\} \tag{3.23}$$

(with φ_0 an arbitrary phase factor). This distribution function is shown in Fig. 6 (first panel) and it corresponds to the Nelson-Toner cubatic phase.

To minimize the free energy we first set $\varphi = \varphi^*$ in Eq. (3.20). The remaining dependence of $[\beta F_4(A,\varphi^*)/2\pi\phi]$ on the amplitude A is a standard Landau order-parameter expansion of the free energy near a first-order phase transition. We conclude that Eq. (3.20) describes a first-order phase transition from an isotropic to a cubatic phase with A as the order parameter.

3. Cubatic-nematic coupling and the tetratic phase

We now allow all terms up to quartic order of *both* $l=2$ and $l=4$ symmetry, but we exclude the $A_{4,2}$ and $A_{2,2}$ coefficients that we found to be zero when minimizing the purely

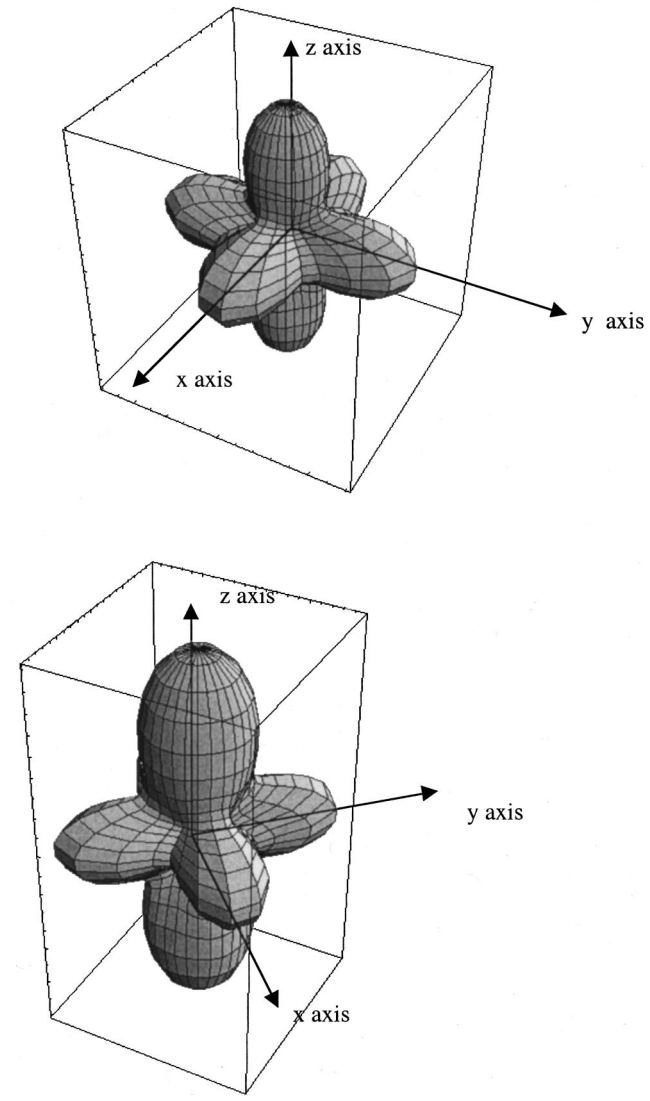

FIG. 6. Orientational distribution functions of the cubatic phase (top panel) and the tetratic phase (bottom panel).

$l=2$ and $l=4$ parts of the free energy. The following cubatic-nematic coupling term is then encountered to first order in the nematic order parameter $A_{2,0}$:

$$\frac{\beta F_{2+4}}{2\pi\phi}=\frac{\beta F_2}{2\pi\phi}+\frac{\beta F_4}{2\pi\phi}+A_{2,0}\sqrt{5}\left\{-\sqrt{\pi}\frac{40}{77}+4\pi\frac{360}{1001}A_{4,0}\right\}\times\left((A_{4,0})^2-\frac{14}{5}|A_{4,4}|^2\right)+(\text{higher-order terms}). \tag{3.24}$$

It follows from Eq. (3.24) that nonzero values of the nematic order parameter are *not* automatically produced whenever $A_{4,0}$ appears. The term $A_{2,0}[(A_{4,0})^2-\frac{14}{5}|A_{4,4}|^2]$ vanishes when $A_{4,4}/A_{4,0}=\sqrt{\frac{5}{14}}$, i.e., precisely at the magical angle that defines the cubatic phase so cubatic order does not impose nematic order.

Higher order coupling terms in $A_{2,0}$ that play a role, but that are not exhibited in Eq. (3.24), are of the form $A_{4,0}(A_{2,0})^2$. These terms guarantee that nonzero values of $A_{4,0}$ are associated with nonzero values of $A_{2,0}$. This is, however, a well-known effect: the actual nematic orientational distribution function is not really a Y_2^0 spherical harmonic (a complete series of the spherical harmonics $Y_1^0(\theta)$ for all even l is required [27]).

The cubatic-nematic coupling term has important consequences. Consider the limiting case $r_2\gg 0$. Far from the nematic instability line, $A_{2,0}$ must in general be small, so we need only to retain linear or quadratic terms in $A_{2,0}$ in Eqs. (3.17) and (3.24). We can write the dependence of the free energy on $A_{2,0}$ in that limit as

$$\frac{\beta F_{cop}(A_{2,0})}{2\pi\phi}\cong\sqrt{5}\left\{-\sqrt{\pi}\frac{40}{77}+4\pi\frac{360}{1001}A_{4,0}\right\}\times\left(A_{4,0}^2-\frac{14}{5}|A_{4,4}|^2\right)A_{2,0}+r_2|A_{2,0}|^2. \tag{3.25}$$

We can minimize Eq. (3.25) with respect to $A_{2,0}$ to obtain a new contribution to the cubatic variational free energy that is quartic in the cubatic order parameter,

$$\frac{\beta F_{cop}(A,\varphi)}{2\pi\phi}=-\frac{\Gamma}{r_2}\left((\cos\varphi)^2-\frac{7}{5}(\sin\varphi)^2\right)^2A^4, \tag{3.26}$$

with Γ a positive numerical constant. This nematic-cubatic coupling term can be absorbed into the cubatic free energy by a redefinition of the function $G(\varphi)$ [see Eq. (3.22)],

$$G^*(\varphi)=G(\varphi)-\frac{\Gamma}{r_2}\left((\cos\varphi)^2-\frac{7}{5}(\sin\varphi)^2\right)^2. \tag{3.27}$$

The second term of $G^*(\varphi)$ in Eq. (3.27) has a *maximum* at the magical angle $\varphi^*=\arctan\sqrt{\frac{5}{7}}$. For large values of r_2, $\varphi^*=\arctan\sqrt{\frac{5}{7}}$ remains the overall minimum of $G^*(\varphi)$, but as we reduce r_2 the minimum turns into a maximum a critical value of r_2 of the order one, as is evident from Eq. (3.27). The free energy acquires a new minimum with ϕ different from ϕ^*. As we continue to reduce r_2 the minimum shifts continuously away from ϕ^*. To interpret the nature of this transition, first note that when ϕ does not equal ϕ^*, then the nematic order parameter $A_{2,0}$ must be finite. That does not mean, however, that the new phase is just a nematic, only that it is birefringent. This is because the new optimal angle ϕ^* is in general not equal to zero or π, which means that the expansion co-efficient $A_{4,4}$ remains nonzero [see Eq. (3.19)]. This, in turn, implies *that the new phase does not have uniaxial symmetry*. A plot of the orientational distribution function is shown in the second panel of Fig. 6: the new phase is a cubatic with a tetragonal distortion along one of the axes. We will call this birefringent phase—with combined nonzero nematic and cubatic order parameters—a ''*tetratic*'' phase since it represents a tetragonal distortion of the cubatic phase. Unlike the cubatic phase, the tetratic phase is birefringent. Figure 7 shows the structure of the phase

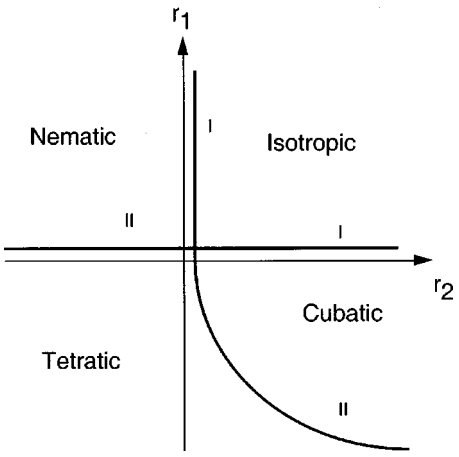

FIG. 7. Mean-field phase diagram near the multicritical point as computed by the numerical minimization of Eq. (3.24).

diagram as obtained by numerical minimization of Eq. (3.24). Note that there is never a direct transition from the cubatic to the nematic and that the four phases appear to come together at a multicritical point. A significant part of the cubatic phase is transformed to a tetratic phase.

It is useful to briefly discuss the nature of the cubatic-to-tetratic transition in a different manner. The proper order parameter describing the appearance of nematic birefringence in an isotropic fluid is not really $A_{2,0}$ but rather Q_{ij}, the anisotropic, traceless part of the dielectric tensor. In a nematic, this tensor has the form

$$Q_{ij}=S(n_i n_j-1/3\delta_{ij}) \tag{3.28}$$

with S the amplitude of the nematic order parameter and with n_i a unit vector along the direction of the optical axis. Because of rotational symmetry, the Landau free energy of the nematic-to-isotropic transition cannot depend on the director orientation and has the form $F(S)=(1/2)rS^2-wS^3+uS^4$ to fourth order in S, with r, w, and u expansion coefficients (there can be no linear terms S since Q_{ij} is traceless). Reducing the coefficient r, we encounter the expected first-order phase isotropic-nematic phase transition.

For the onset of birefringence in a *cubatic* environment, we must allow for terms that are dependent on the director orientation. Cubic symmetry permits the following second-order terms:

$$F_2=\tfrac{1}{2}\,\lambda_{xxxx}(Q_{xx}^2+Q_{yy}^2+Q_{zz}^2)+\lambda_{xxyy}(Q_{xx}Q_{yy}+Q_{xx}Q_{zz}+Q_{yy}Q_{zz})+2\lambda_{xyxy}(Q_{xy}^2+Q_{xz}^2+Q_{yz}^2). \tag{3.29}$$

The three λ parameters are coefficients of a tensor of rank four with cubic symmetry. In terms of the amplitude S and the director, this expression simplifies to

$$F_2=\tfrac{1}{2}\,rS^2+\tfrac{1}{2}\,(\lambda_{xxxx}-\lambda_{xxyy}-2\lambda_{xyxy})S^2(n_x^4+n_y^4+n_z^4) \tag{3.30}$$

with r a linear combination of the λ parameters. The second term of Eq. (3.30) must be zero if there is no cubatic order so, to lowest order, it must be proportional to the cubatic order parameter A

$$(\lambda_{xxxx}-\lambda_{xxyy}-2\lambda_{xyxy})=aA. \tag{3.31}$$

From the previous discussion, we know that the preferential direction of the optical axis should be along one of the cubatic directions. This conditions demands that the coefficient a in Eq. (3.31) is negative. The free energy is then minimized if the optical axis of the tetratic phase lies along one of the cubatic axes. Choosing the optical axis along any of the three cubatic axes, we recover the same form for $F(S)$ but with the expansion parameter r replaced by $r+aA$. The onset of birefringence in a cubatic thus should remain a first-order transition but the larger the cubatic order parameter A, the earlier birefringence starts when we reduce r, consistent with Fig. 7.

IV. PHASE COEXISTENCE

The exotic liquid-crystal phases appear along the border of a region of phase decomposition. The fact that network formation by cross-linked polymers can be accompanied by phase separation is well established [28] for the case that angle-dependent forces play no role. Two physical considerations play here an important role. First, when a certain concentration of (strong) linkers is added to a solution of polymers, then extended networks appear for increasing linker concentration when we cross the *percolation threshold* (see Fig. 1). For rigid rods, the linker concentration at the percolation threshold is proportional to the rod concentration ϕ, with a proportionality constant close to two. We can view the control parameter $e^{\beta\Delta F_0}$ of Sec. III as the probability for the formation of a link on a rod, so the percolation criterion for network formation is similar to the condition that $e^{\beta\Delta F_0}$ must exceed a critical value for the formation of a dilute aggregate.

Next, assume that the initial linker-free rod concentration is high enough so the starting solution is at least *semidilute*. This means that there are a certain number of ''preexisting'' contacts between the rods. Let $\xi(\phi)$ be the correlation length of the semidilute solution [$\xi(\phi)$ is proportional to $(1/\phi)^{1/2}$ as discussed below]. The concentration of these contacts is then proportional to $1/(\xi(\phi))^3$. If the linker concentration is *less* than the concentration of native contacts, then all linkers can be accommodated by the semidilute solution with no change in local structure. When the linker concentration exceeds the concentration of preexisting contacts then this forces a decrease of the correlation length to a value below the one of the semidilute solution. This results in a significant reduction of the entropy of the semidilute solution. This free energy increase can be avoided by absorbing the excess linkers into *dense clusters* containing only a limited number of rods and many linkers, a form of phase separation known as ''microgelation.'' Note that these dense clusters are compacted by entropy: releasing rods from the clusters into the solution increases the entropy of the system.

We now will examine the nature of the phase-separation in more detail for the present case where the rods are charged and where polyvalent ions act as cross-linkers.

A. Isotropic-cubatic phase coexistence ($\psi/\phi < \kappa L$)

First consider a state where a linker-rich network coexists with a linker-poor isotropic rod solution restricting ourselves for simplicity to the case that the network phase is a cubatic aggregate and that (nearly) all the linker ions, M in number, are absorbed by the cubic network. Let the characteristic mesh size of the aggregate be ξ, the aggregate rod volume fraction Φ, and the aggregate volume V_a (assumed small compared to the total sample volume V). The rod concentration ϕ_a of the aggregate is then equal to Φ/Ω with Ω, of order LD^2, the rod volume. The aggregate volume fraction Φ is related to the mesh size ξ, the linker number M, and to V_a by simple geometrical relations,

$$V_a \propto M\xi^3, \tag{4.1a}$$

$$\Phi \propto \left(\frac{D}{\xi}\right)^2. \tag{4.1b}$$

To treat the phase separation, we must generalize the Onsager variational free energy of Sec. III. A mechanism is required that restrains the uncontrolled growth of the rod concentration when we cross the boundary of the dense and/or dilute phase coexistence region. This physical mechanism is, for low salt concentrations, electrostatic repulsion between the rods. The variational free energy for a sample exhibiting isotropic and/or cubatic phase coexistence in the presence of electrostatic repulsion is

$$\Delta F/Vk_BT \approx \phi_s \ln(\phi_s \nu_T) + (V_a/V)\Big\{\phi_a \ln(\phi_a \nu_T) + c_1\phi_a \ln(c_2\phi_a L^2 D) + c_3\frac{L}{l_B}\phi_a K_0(\kappa\xi)\Big\}. \tag{4.2}$$

The first term is the entropic free energy of the isotropic solution. The rod concentration of the isotropic solution is ϕ_s (we neglect the second-order virial terms for the isotropic solutions). Conservation of the number of rods requires that

$$V\phi_s + V_a\phi_a = V\phi. \tag{4.3}$$

The second term of Eq. (4.2) is the free energy of the aggregate. The first two terms inside the brackets are the translational and rotational entropic free energies of the cubatic phase obtained above [see Eqs. (3.8) and (3.11); c_1 and c_2 are constants]. The third term inside the curly brackets describes the electrostatic repulsion—computed within DH theory—between the rods of a cubatic structure of mesh size ξ. K_0 is the modified Bessel function and c_3 is a positive constant. Since the mesh size depends on the rod concentration ϕ_a through Eq. (4.1), Eq. (4.2) is indeed nonlinear. In the limit that the aggregate contains only a small fraction of all the rods, i.e., that $V_a\phi_a \ll V\phi$, we can expand Eq. (4.2) in powers of the ratio $V_a\phi_a/V\phi$ with the following result:

$$\Delta F\Omega/k_BT \approx V\phi\Omega \ln(\phi\nu_T) + M\frac{D^3}{\Phi^{1/2}}\left(\ln(\Phi/\Omega\phi) + c_1\ln(c_2\Phi L/D) + c_3\frac{L}{l_B}K_0(\kappa D/\Phi^{1/2})\right). \tag{4.4}$$

We will minimize the free energy with respect to Φ for fixed M under the constraints of Eqs. (4.1) and (4.3). The first two terms inside the large parentheses favor large Φ. This is just the entropic-compaction mechanism: by increasing Φ we can release rods and hence reduce the overall free energy of the mixture. The last term in large parentheses is negligible as long as the mesh size ξ is large compared to the Debye length $1/\kappa$. On the other hand, because the rod length L is large compared to the Bjerrum length l_B this term makes the free-energy cost of any network with ξ much less than the Debye length prohibitively large. We thus expect that compaction continues until the mesh size becomes comparable to the Debye screening length (at least for $\kappa D \ll 1$). Explicit minimization of Eq. (4.4) gives

$$\Phi^* \approx \left(\frac{\kappa D}{\ln(L/l_B)}\right)^2. \tag{4.5}$$

Comparing with Eq. (4.1b) it is easy to show that this result is consistent with our intuition that $\kappa\xi$ is of order one.

As we increase the linker concentration ψ, the aggregate volume grows further by incorporating more and more rods and eventually we exhaust the uniform solution. This happens when $V_a\phi_a/V\phi$ is of order one. Using this criterion together with Eqs. (4.1) and (4.5), we find that the maximum linker to the rod concentration ψ/ϕ for which coexistence between an isotropic phase and a cubatic phase remains possible is of order κL. This is just the condition for the mean spacing between the links of a network containing *all* the rods to be equal to the Debye screening length.

B. Dense bundle–cubatic phase coexistence ($\psi/\phi > \kappa L$)

We saw that when ψ/ϕ is large compared to κL, phase coexistence between a cubatic network and an isotropic solution no longer is possible. A new form of phase decomposition is required with one of the two phases accommodating a higher density of linkers than the cubatic phase is capable of. Such a phase exists: the dense bundle discussed in the Introduction. In its simplest form, a dense bundle is charge neutral: polyvalent ions cancel the charges of the rods, allowing the rods to be in close proximity. The essential point is thus that dense bundles can absorb far more polyvalent ions than the network phase. These polyvalent ions are either condensed into a Wigner crystal, or they may remain mobile forming a highly correlated liquid. Numerical simulations of pairs [29] or bundles [14] of polyelectrolyte rods indicate that, at room temperature, divalent ions are still fairly mobile.

The preceding argument would suggest that the most natural form of phase coexistence would be to use *all* the polyvalent ions to construct a charge-neutral dense bundle, with the remaining rods free to form a linker-free isotropic or nematic phase. As long as we are far from the isoelectric point, the bundle needs to absorb only a small fraction of the total number rods to cancel the linker charge. This may not be true, however. Suppose we remove a polyvalent ion from the bundle and use it to create a link between two rods in solution. The local electrostatic energy of the ion should not be much affected by the transfer—the ion is sandwiches between two rods in either case—but this is not true for the *entropy* of the system. Transfer of a polyvalent ion of valence Z out of the bundle should permit release of Z counterions out of the Manning clouds of the two rods. Studies of counterion release under different circumstances [30] show that this process should lower the entropic free energy of the system by, approximately, k_BT per released ion. This counterion release mechanism is opposed by the free-energy cost incurred by the electrical charging of the bundle due to the removal of the polyvalent ion [31]. This argument would lead to the conclusion that dense *bundles may be spontaneously charged*. The excess ions are used as cross-linkers in solution and may form a network.

To estimate the free-energy cost of transferring ions from a bundle to the rods in solution, we will perform the transfer process in steps. First, we remove M polyvalent ions of valence Z from a very long, charge-neutral cylindrical bundle of radius R_b. To compute the *capacitive charging free energy* $\Delta F_{\rm cap}$ of the bundle, we first note that the remaining, mobile polyvalent ions of the bundle must redistribute themselves until a state of equilibrium is reached in which there is no net electrical field in the interior of the dense bundle. It follows from Gauss's law that in this equilibrium state the interior must be charge neutral, so the total charge ZM of the dense bundle must be distributed uniformly over the *surface* of the cylinder.

The average surface charge area density of the dense bundle is thus $\sigma=-MZ/A_b$, with A_b, the surface area of the bundle. The Poisson-Boltzmann (PB) free energy per unit area of a *flat* charged surface with a fixed surface charge density σ is given by [32]

$$\gamma(\sigma)=|\sigma|k_BT\ln\left(\frac{l_B\sigma^2}{2c_0}\right) \tag{4.6}$$

in the limit of no added salt (c_0 is a normalization constant that will later drop out). Using Eq. (4.6), the charging free-energy cost of the bundle is estimated as

$$\Delta F_{\rm cap}(M)=MZk_BT\ln\left(\frac{l_B(MZ/A_b)^2}{2c_0}\right)+M\Delta H_{\rm bundle}, \tag{4.7}$$

with $\Delta H_{\rm bundle}$ the contribution to the capacitive charging energy cost by the *local* electrostatic correlation energy of the bundle. (Neglecting the curvature of the bundle should be permitted provided R_b is large compared with the characteristic width of the charge cloud surrounding the dense bundle, which is the Chapman length $(l_B\sigma)^{-1}=A_B/l_BMZ$.)

The next step is to place M polyvalent ions on the surface of free rods in solution. This leads to an effective partial discharge of the rods and the release of MZ monovalent ions. The free-energy gain obtained by counterion release is, within PB theory [33]

$$\Delta f_{\rm rel}\cong k_BT\ln\left(\frac{\xi_M}{2\pi c_0bD^2}\right) \tag{4.8}$$

per released ion (for the case of no added salt). In Eq. (4.8), D is the rod diameter, $1/b$ is the line density of charges along the rod, and ξ_M is the Manning parameter [i.e., $\xi_M=l_B/b$; Eq. (4.8) is the limit case of $\xi_M\ll 1$]. The normalization constant c_0 is the same as in Eq. (4.7). The discharge energy of the rods is then

$$\Delta F_{\rm rod}=-M(\Delta f_{\rm ret}+\Delta H_{\rm rod}) \tag{4.9}$$

with $\Delta H_{\rm rod}$ the contribution to the electrostatic free-energy gain due to interaction of the polyvalent ion with local charges of the rod (which is also beyond PB theory).

Finally, we construct M single-ion salt bridges between free rods. The free energy per gain per bridge is taken to be $\Delta F_1(\gamma=\pi/2)$. The total free energy change of the charge transfer process is then

$$\Delta F(M)/k_BT\approx M\Delta H-MZ\ln\left(\frac{\xi_M}{2\pi c_0bD^2}\right)+MZ\ln\left(\frac{l_B(MZ/A_b)^2}{2c_0}\right), \tag{4.10}$$

with

$$\Delta H=\Delta H_{\rm bundle}-\Delta H_{\rm rod}-\Delta F_1(\gamma=\pi/2). \tag{4.11}$$

The quantity ΔH represents the local free-energy cost of transforming a polyvalent ion inside a dense bundle into an ion link in a rod network. If we accept the fact that the local electrostatic environment of a polyvalent ion inside a bundle is similar to that of an ion link between two rods in solution, then ΔH should be modest (i.e., of order k_BT). Minimizing $\Delta F(M)$ with respect to M gives the following equilibrium number of cross-links:

$$M^*\approx\frac{A_B}{ZDb}e^{-\beta\Delta H/2Z}. \tag{4.12}$$

The surprise is that the number of released polyvalent ions is determined by the *surface area* of the dense bundle.

We now can use Eq. (4.12) to determine under which conditions the dense bundle releases a sufficient number of polyvalent ions to transform the remaining free rods into a network phase (of the type discussed in Sec. II). The number of polyvalent ions in a fully charged neutral cylindrical bundle of length L_b is of order $L_bR_b^2/(ZD^2b)$, since ZD^2b is the volume per polyvalent ion. The fraction δ of all polyva-

lent ions that is transferred back into solution out of the dense bundle is then the ratio of M^* and $L_b R_b^2/(ZD^2 b)$,

$$\delta \approx \frac{D}{R_b} e^{-\beta \Delta H/2Z}, \tag{4.13}$$

with A_b of order $L_b R_b$. The concentration of released linkers in solution is $\delta\psi$ since ψ was the original concentration of linkers. By assumption, the dense bundle contains only a small fraction of all rods, so the linker-to-rod concentration ratio of the free rods in solution is of order $\delta\psi/\phi$. Recall that the crude (percolation) criterion for network formation by strong linkers is that the linker-to-rod concentration ratio must be larger than a number of order one. We saw earlier that ψ/ϕ had to be of order κL at the onset of bundle formation. It follows that $\delta\kappa L$ must be larger than one in order for network formation to be possible at the onset of bundle formation. Using Eq. (4.13), this condition translates to

$$\frac{D\kappa L}{R_b} e^{-\beta \Delta H/2Z} \geqslant O(1). \tag{4.14}$$

Physically, this effect may be viewed as the electrochemical competition for monovalent ions between the ''thin'' charged rods of diameter D—the polyelectrolytes in solution—and ''thick'' charged rods—the cylindrical dense bundle of diameter R_b. By allowing the bundle to charge up through the removal of polyvalent ions, we can transfer monovalent ions from the surface of the thin rods to the surface of the thick rod, which lowers their density and hence increases their entropy.

V. CONCLUSION

The central result of this paper is that elementary statistical mechanics arguments indicate that under generic conditions exotic mesophases will form if we mix charged rigid rods with small polyvalent counterions. It is important to realize the limitations of the methods when discussing its predictions. The most serious limitation is the ''Onsager'' restriction of the free-energy variational expression Eq. (3.1) to second-order virial terms. For instance, when mixtures of hard rods and hard spheres are examined experimentally, complex forms of microphase transitions are observed [34] that do not readily follow from Onsager theory. In such mixtures, *smectic*like structures are encountered, and smecticlike structures actually might be present in the actin experiments that were described in the Introduction [35].

The next concern is that even within a second-order virial expansion, we do not have a very accurate form for important quantities such as $\Delta F_{1,2}(\gamma)$ and $V(\gamma)$. This would require numerical simulations of the counterion distribution near a cross-link taking into account the actual molecular environment of the biopolymers in question. Since the two biopolymers are in close vicinity near a link, the molecular structure of the polymers is expected to be important in determining $V(\gamma)$. We argued in Sec. III that the symmetry of the exotic mesophases *at onset* should not depend sensitively on the precise structure of $V(\gamma)$, only on the angle γ^* where $V(\gamma)$ turns negative. However, as the minimum deepens the details of $V(\gamma)$ certainly will start to play a larger role. In particular, two ion-linked biopolymers are not likely to assume the 90° orientation of the single-ion link of our simple model. In a recent DH calculation of the function $U(\gamma,R)$ for two crossing DNA strands, Kornyshev and Leikin [36] obtained a complex structure for $U(\gamma,R)$ with *small* optimal crossing angles γ^* of order $(PD)^{1/2}/L$ (P is the helical pitch of DNA). It is in fact possible to study γ^* experimentally by attaching two double-stranded DNA molecules together at a single point by crosswise exchange of single strands (''Holliday junction''). Confusingly, in the absence of polyvalent salt ions, a Holliday junction appears to have a large crossing angle near 90°, while in the presence of finite concentrations of Mg^{2+} ions, the angle reduces from 90° to about 60° [37], which actually would be in accord with the results of Sec. III. In any case, it is clear that an accurate determination of $V(\gamma)$ would be very useful to make further progress.

Next, we neglected thermal fluctuations. For the phase behavior of very long, stiff rods such as actin, this is probably not an important limitation but for biopolymers with shorter persistence lengths, such as DNA, thermal fluctuations are likely to become increasingly important. If the persistence length drops below the Debye screening length—and hence the mesh size—then we should expect that thermal fluctuations could significantly alter the internal structure of the network phase. The effect of thermal fluctuations on the tetratic phase could be rather interesting. Strong thermal fluctuations might, for instance, lead to phase fluctuations that transform the tetratic phase into a nematic phase with an unusual structure factor. Finally, we did not include chirality. DNA is, for instance, well known to exhibit a cholesteric phase [38], with the rod direction perpendicular to the chiral axis. If we would increase the chiral nature of the interaction, then exotic *chiral* mesophases may become possible, for instance the analog of the tetratic phase with the phase factor φ_0 in Eq. (3.31) now z dependent [e.g., $\varphi_0(z) = 2\pi(z/P)$]. These phases would compete with the cholesteric phase rather than with the nematic phase. The dense bundle phase also may acquire a chiral character [18].

This paper was motivated by the experiments of Ref. [16]. To what extent can we now interpret these results? For 90° crossing angles, we encountered only one birefringent network phase: the tetratic phase. The structure factor of a tetratic network phase of semiflexible polyelectrolytes can be shown to have separate maxima both along the directions parallel and perpendicular to the optical axis at different positions, consistent with the measured structure factor. It thus seems indeed possible that the network phase of Ref. [16] either is a tetratic liquid crystal or a tetragonal crystal but the precise peak positions of $S(q)$ appear to be different from that expected of a tetratic phase [39]. Under conditions of phase coexistence of network and isotropic material, the characteristic mesh size of the network is predicted to be the Debye screening length which is not inconsistent with the experiments of Ref. [16]. Finally, can the network be in electrochemical equilibrium with dense bundles? The numerical simulations [14] on semiflexible polyelectrolytes report that the ratio of D/R_b is of order 10^{-2}. If we use this estimate in

Eq. (4.14) and assume that ΔH is of order ZkT or less, then electrochemical equilibrium is possible between a network and a bundle phase when κL is of order 10^2 or larger. This condition appears to be satisfied by the experiment of Ref. [16].

An interesting issue we did not discuss concerns the *elastic properties* of the mesophases. As mentioned, the rheology of actin solutions has been the subject of intense interest. The elastic properties of the birefringent network phases might be unusual. For instance, both traction and shear stress may cause the birefringent axis of the tetratic phase to rotate, given sufficient time. It would also be interesting to see how the relative balance between the network phase and the isotropic solution and between the network phase and the bundle phase is effected by external elastic stress. Osmotic pressure should favor the bundle phase over the network phase and hence alter the phase coexistence.

ACKNOWLEDGMENTS

I would like to thank C. Safinya for suggesting this study, for showing me unpublished data, and for a critical reading of the manuscript. I would like to thank G. Wong for a critical reading of the manuscript and W. Gelbart, A. Liu, and T. Lubensky for helpful conversations. I would like to acknowledge support from the Rothschild Foundation and from NSF Grant No. DMR-9407741.

[1] L. Onsager, Ann. N.Y. Acad. Sci. **51**, 627 (1949).

[2] G. C. Berry, P. M. Cotts, and S. G. Chu, Polym. J. (Tokyo) **13**, 47 (1981); S. Yue, G. C. Berry, and M. M. Green, Polym. Prepr. (Am. Chem. Soc. Div. Polym. Chem.) **23**, 529 (1991); C. Wei-Berk and G. C. Berry, J. Appl. Polym. Sci. **45**, 261 (1990).

[3] P. van der Schoot, Ph.D. thesis, University of Delft, 1992, Ch. VII. See also P. van der Schoot and T. Odijk, J. Chem. Phys. **97**, 515 (1992).

[4] For an introductory review to the physical aspects of actin polymers, see the following website by P. Janmey, J. Tang, and C. Schmidt: http://expmed.bwh.harvard.edu/projects/polymer/actin_chapter/index.htm.

[5] C. Coppin and P. Leavis, Biophys. J. **63**, 794 (1992); R. Furukawa, R. Kundra, and M. Fechheimer, Biochemistry **32**, 12 346 (1993); J. Kas *et al.*, Biophys. J. **70**, 609 (1996); P. Das, J. Xu, J. Roy, and N. Chakrabarti, J. Chem. Phys. **111**, 8240 (1999).

[6] A. Stroobants, H. N. M. Lekkerkerker, and T. Odijk, Macromolecules **19**, 2232 (1986); Z. Y. Chen, *ibid.* **26**, 3419 (1993); J. Tang and S. Fraden, Liq. Cryst. **19**, 459 (1995).

[7] P. Janmey, S. Hvidt, J. Lamb, and T. Stossel, Nature (London) **345**, 89 (1990).

[8] M. Tempel, G. Isenberg, and E. Sackmann, Phys. Rev. E **54**, 1802 (1996); A. Palmer, J. Xu, and D. Wirtz, Rheol. Acta **37**, 97 (1998).

[9] For measurements of the rheological properties of actin, see B. Hinner *et al.*, Phys. Rev. Lett. **81**, 2614 (1998); J. Kas *et al.*, Biophys. J. **70**, 609 (1996).

[10] F. MacKintosh, J. Kas, and P. Janmey, Phys. Rev. Lett. **75**, 4425 (1995); R. Everaers, F. Julicher, A. Ajdari, and A. Maggs, *ibid.* **82**, 3717 (1999); H. Isambert and A. Maggs, Macromolecules **29**, 1036 (1996); D. C. Morse, Phys. Rev. E **58**, 1237 (1998).

[11] For an introduction to the effects of actin cross-linking on cell motility, T. Stossel, Sci. Am. 54 (September, 1994).

[12] V. A. Bloomfield, Curr. Opin. Struct. Biol. **6**, 334 (1996); J. Tang and P. Janmey, J. Biol. Chem. **271**, 8556 (1996); J. Tang *et al.*, Biochemistry **36**, 12 600 (1997).

[13] N. Gronbech-Jensen, R. Mashl, R. Bruinsma, and W. Gelbart, Phys. Rev. Lett. **78**, 2477 (1997).

[14] M. Stevens, Phys. Rev. Lett. **82**, 101 (1999).

[15] B. Y. Ha and A. J. Liu, Europhys. Lett. **46**, 624 (1999).

[16] G. Wong, Y. Li, and C. Safinya (unpublished).

[17] J. V. Selinger and R. F. Bruinsma, Phys. Rev. A **43**, 2910 (1991).

[18] R. Kamien and D. Nelson, Phys. Rev. Lett. **74**, 2499 (1995).

[19] P.-G. de Gennes, P. Pincus, R. Velasco, and F. Brochard, J. Phys. (Paris) **37**, 1461 (1976).

[20] R. Blaak (unpublished). See also J. A. C. Veerman and D. Frenkel, Phys. Rev. A **45**, 5632 (1992).

[21] D. Nelson and J. Toner, Phys. Rev. B **24**, 363 (1981); P. J. Steinhardt, D. R. Nelson, and M. Ronchetti, *ibid.* **28**, 784 (1983).

[22] The tetratic phase is very similar to the $N+6$ phase introduced by J. Toner, Phys. Rev. A **27**, 1157 (1983), and would in fact correspond to the $N+4$ phase.

[23] F. Oosawa, J. Polym. Sci. **23**, 421 (1957); G. S. Manning, J. Chem. Phys. **51**, 924 (1969); **51**, 3249 (1969); G. S. Manning, Q. Rev. Biophys. **11**, 179 (1978); M. LeBret and B. Zimm, Biopolymers **23**, 287 (1984); D. Stigter, Biophys. J. **69**, 380 (1995).

[24] S. L. Brenner and V. A. Parsegian, Biophys. J. **14**, 327 (1974).

[25] Expansion in spherical harmonics of the distribution function is a standard technique, G. Luckhurst and G. Gray, *The Molecular Physics of Liquid Crystals* (Academic Press, London, 1978). The only difference is that we keep the nonzero m terms. By choosing preferred axes, this representation is not suitable for discussing issues involving the rotational invariance of the free energy.

[26] This assumption may be questionable if end effects are important.

[27] R. L. Humphries, P. G. James, and G. R. Luckhurst, J. Chem. Soc., Faraday Trans. 2 **68**, 1031 (1972); G. R. Luckhurst and F. R. Viloria, Mol. Cryst. Liq. Cryst. Lett. **72**, 201 (1982).

[28] See T. Miura, H. Okumoto, and H. Ichijo, Phys. Rev. E **54**, 6596 (1996), and references therein.

[29] N. Gronbech-Jensen, R. Mashl, R. Bruinsma, and W. Gelbart, Phys. Rev. Lett. **78**, 2477 (1997).

[30] P. de Haseth, T. Lohman, and T. Record, Biochemistry **16**, 4783 (1977); C. F. Anderson and M. T. Record, J. Phys. Chem. **97**, 7116 (1993), and references therein.

[31] A very similar problem is encountered in the complexation of DNA with histones. See S. Y. Park, R. Bruinsma, and W. Gelbart, Europhys. Lett. **46**, 454 (1999).
[32] See, for instance, W. M. Gelbart and R. Bruinsma, Phys. Rev. E **55**, 831 (1997) and references therein.
[33] F. Oosawa, *Polyelectrolytes* (Dekker, New York, 1971).
[34] M. Adama, Z. Dogic, S. Keller, and S. Fraden, Nature (London) **393**, 349 (1998).
[35] C. Safinya (private communication).
[36] A. A. Kornyshev and S. Leikin (unpublished).
[37] D. Lilley and R. Clegg, Q. Rev. Biophys. **26**, 131 (1993); N. Seeman and N. Kallenbach, Annu. Rev. Biophys. Biomol. Struct. **23**, 53 (1994).
[38] D. Durand, J. Doucet, and F. Livolant, J. Phys. II **2**, 1769 (1992); K. Kassapidou and J. R. C. van der Maarel, Eur. Phys. J. B **3**, 471 (1998); K. Merchant and R. L. Rill, Biophys. J. **73**, 3154 (1997).
[39] C. Safinya (private communication).